Semiannual Technical Report

Pseudomorphic Semiconducting Heterostructures from Combinations of AlN, GaN and Selected SiC Polytypes: Theoretical Advancement and its Coordination with Experimental Studies of Nucleation, Growth, Characterization and Device Development

Supported under Grant #N00014-90-J-1427
Office of the Chief of Naval Research
Report for the period 1/1/95–6/30/95

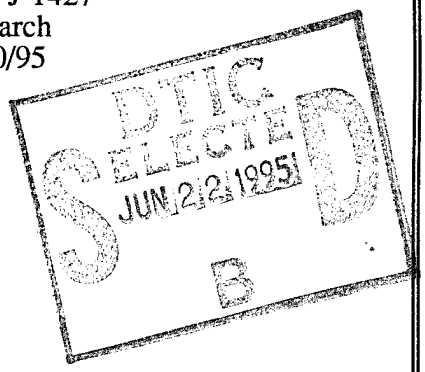

R. F. Davis, O. Aboelfotoh, S. Kern, K. Linthicum and J. Sumakeris
Materials Science and Engineering Department
North Carolina State University
Campus Box 7907
Raleigh, NC 27695-7907

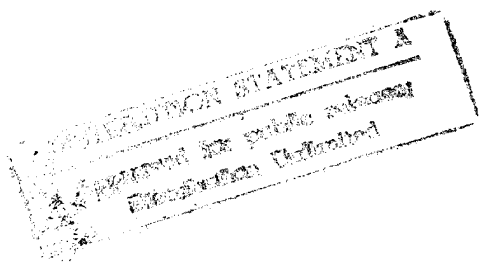

June, 1995

REPORT DOCUMENTATION PAGE

Form Approved
OMB No. 0704-0188

1. AGENCY USE ONLY *(Leave blank)*	2. REPORT DATE	3. REPORT TYPE AND DATES COVERED
	June, 1995	Semiannual Technical 1/1/95–6/30/95

4. TITLE AND SUBTITLE

Pseudomorphic Semiconducting Heterostructures from Combinations of AlN, GaN and Selected SiC Polytypes: Theoretical Advancement and its Coordination with Experimental Studies of Nucleation, Growth, Characterization and Device Development

5. FUNDING NUMBERS

414s007---01
1114SS
N00179
N66005
4B855

6. AUTHOR(S)

Robert F. Davis

7. PERFORMING ORGANIZATION NAME(S) AND ADDRESS(ES)

North Carolina State University
Hillsborough Street
Raleigh, NC 27695

8. PERFORMING ORGANIZATION REPORT NUMBER

N00014-90-J-1427

9. SPONSORING/MONITORING AGENCY NAMES(S) AND ADDRESS(ES)

Sponsoring: ONR, Code 312, 800 N. Quincy, Arlington, VA 22217-5660
Monitoring: Administrative Contracting Officer, Regional Office Atlanta
Regional Office Atlanta, 101 Marietta Tower, Suite 2805
101 Marietta Street
Atlanta, GA 30332-0490

10. SPONSORING/MONITORING AGENCY REPORT NUMBER

11. SUPPLEMENTARY NOTES

12a. DISTRIBUTION/AVAILABILITY STATEMENT

Approved for Public Release; Distribution Unlimited

12b. DISTRIBUTION CODE

13. ABSTRACT *(Maximum 200 words)*

The use of NH_3 as an alternative to ECR in the gas source(GS) MBE of GaN has resulted in an increase in the growth rate and a sharp peak at 354 nm in the PL spectrum. The use of an ammonia cracker cell was investigated. Stoichiometric GaN films have also been deposited on Al_2O_3(0001), Si(001) and Si(111) substrates using an NH_3 seeded free He jet and an effusive triethylgallium (TEG) source. Very uniform films have been achieved at low temperatures. Work continues toward the construction of a dual supersonic beam deposition system with an attached UHV analysis system. The results of GaN film deposition in the current single beam system and progress toward the completion of the next system are detailed. MIS diodes (Al/AlN/α-SiC(0001)) were fabricated with various thicknesses of AlN by GSMBE. High frequency C-V measurements between 10 kHz and 1 MHz showed that thin layers (<1000Å) of AlN exhibited moderate leakage currents; thicker layers reduced this problem. The diodes could be accumulated and depleted over the entire frequency range studied. Inversion was not achieved at room temperature. A dependence of the dielectric constant on frequency was also observed.

14. SUBJECT TERMS

gallium nitride, GaN, aluminum nitride, AlN, ammonia, molecular beam epitaxy, MBE, MIS diodes, C-V measurements, dielectric constant, supersonic beams

15. NUMBER OF PAGES

21

16. PRICE CODE

17. SECURITY CLASSIFICATION OF REPORT	18. SECURITY CLASSIFICATION OF THIS PAGE	19. SECURITY CLASSIFICATION OF ABSTRACT	20. LIMITATION OF ABSTRACT
UNCLAS	UNCLAS	UNCLAS	SAR

Table of Contents

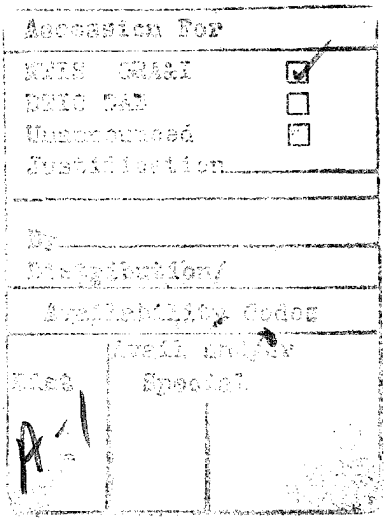

I. Introduction

The advent of techniques for growing semiconductor multilayer structures with layer thicknesses approaching atomic dimensions has provided new systems for both basic physics studies and device applications. Most of the research involving these structures has been restricted to materials with lattice constants that are equal within $\simeq 0.1\%$. However, it is now recognized that interesting and useful pseudomorphic structures can also be grown from a much larger set of materials that have lattice-constant mismatches in the percent range. Moreover, advances in computer hardware and software as well as the development of theoretical structural and molecular models applicable for strained layer nucleation, growth and property prediction have occurred to the extent that the field is poised to expand rapidly. It is within this context that the research described in this report is being conducted. The materials systems of concern include combinations of the direct bandgap materials of AlN and GaN and selected, indirect bandgap SiC polytypes.

The extremes in thermal, mechanical, chemical and electronic properties of SiC allow the types and numbers of current and conceivable applications of this material to be substantial. However, a principal driving force for the current resurgence of interest in this material, as well as AlN and GaN, is their potential as hosts for high power, high temperature microelectronic and optoelectronic devices for use in extreme environments. The availability of thin film heterostructural combinations of these materials will substantially broaden the applications potential for these materials. The pseudomorphic structures produced from these materials will be unique because of their chemistry, their wide bandgaps, the availability of indirect/direct bandgap combinations, their occurrence in cubic and hexagonal forms and the ability to tailor the lattice parameters and, therefore, the amount of strain and the physical properties via solid solutions composed of the three components.

The research conducted in this reporting period and described in the following sections has been concerned with (1) the use of gas source MBE and thermally cracked ammonia to grow AlN and GaN thin films, (2) the development and employment of supersonic jets to grow GaN thin films at low temperatures, and (3) the fabrication by GSMBE and electrical characterization of Al/AlN/SiC MIS diodes. These sections detail the procedures, results, discussions of these results, conclusions and plans for future research. Each subsection is self-contained with its own figures, tables, and references.

II. Growth of AlN and GaN Thin Films via Gas Source Molecular Beam Epitaxy

A. Introduction

Recent research efforts in the wide-bandgap, III-V nitride, semiconductor field have concentrated on the development of light-emitting diodes (LEDs) that emit in the blue spectral region. An AlGaN/InGaN/AlGaN double heterostructure blue LED has been developed in Japan and is now commercially available. The logical next step is the fabrication of blue and UV lasers. The III-V nitrides are most promising candidate materials for these devices because they possess three favorable characteristics: (1) they all have direct transition band structures, (2) their bandgap energies range from the deep UV (6.2 eV (AlN)) to the orange (2.8 eV (InN)) regions of the spectrum, and (3) they can be mixed to form solid solutions allowing for the tailoring of bandgap energies to specific wavelengths.

One of the promising optical devices ideally suited for fabrication using the III-V nitrides is the Vertical Cavity Surface Emitting Laser (VCSEL). VCSELs have significant advantages over edge-emitting lasers for optoelectronic communications. The laser beam emitted from the VCSEL propagates normal to the plane of the substrate, thereby making alignment for chip-to-chip communication much simpler. Additionally, the chip area occupied by a VCSEL is relatively small compared to one required by an edge-emitter [1]. One unique feature of these VCSELs is that both the central light-emitting active region and the outermost distributed Bragg reflectors (DBRs) which form the Fabry-Pérot cavity are all dimensionally defined in one integrated crystal growth sequence performed over the entire wafer using epitaxial techniques such as Molecular Beam Epitaxy (MBE), Gas Source Molecular Beam Epitaxy (GSMBE) and CBE [2]. Efficient performance of such a device requires both high-quality crystalline microstructures and precise control of layer thickness and alloy composition to obtain the highly reflective mirrors and to ensure that the Fabry-Pérot resonance is placed at the exact wavelength for lasing. A typical schematic of a VCSEL structure is shown below. By incorporating a strained MQW active region and by varying the compositional ratios of the group III elements (Al, Ga, and In), the emission wavelength can be tailored to emit in the UV, blue and blue-green spectra.

AlN, GaN and InN thin films are presently grown by various techniques including MOVPE, RF sputtering, and electron cyclotron resonance (ECR) plasma assisted GSMBE. Within the past several years, significant advances in GaN and AlN growth techniques have been achieved [4-12]. Consequently, high quality GaN epitaxial films that exhibit remarkably improved surface morphologies can now be produced by CVD growth techniques. We are currently employing GSMBE to determine the optimal growth parameters for the binary

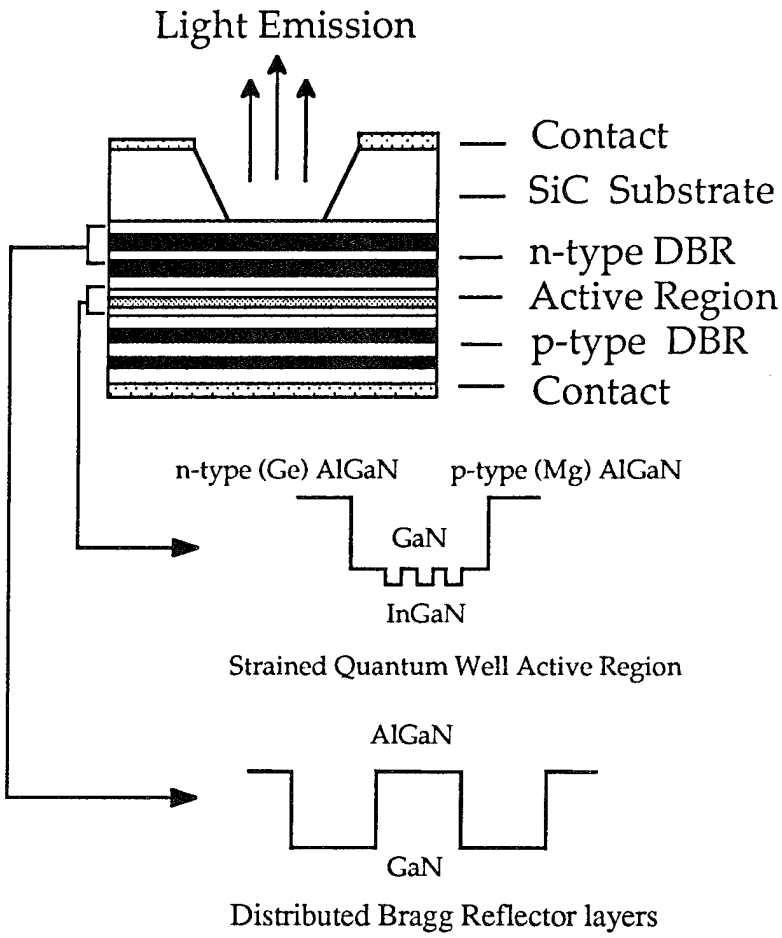

Schematic of a typical VCSEL structure.

compounds, selected solid solutions of these compounds and multilayer heterostructures of these materials in terms of microstructure and optical and electrical properties. Additionally, researchers have successfully doped the III-V nitrides and their alloys creating n-type (Si, Ge) doped films [13-15] and more notably, p-type magnesium doped films [6,11,14]. Although these recent developments have provided all of the material ingredients necessary for the fabrication of efficient LEDs, further refinement in film quality, namely GaN and InN, is still needed for the GSMBE growth and fabrication of VCSEL structures. This report presents the current research aimed at optimizing the microcrystalline and optical quality of GaN by employing thermally cracked ammonia as an alternative to our ECR plasma source used in III-V nitride thin-film growth.

B. Experimental Procedure

GaN and AlN thin-films were grown on (0001) oriented α(6H)-SiC wafers provided by Cree Research, Inc. The films were grown by GSMBE using a commercial Perkin-Elmer 430 system. The Al and Ga fluxes were provided by standard Knudson effusion cells. Nitride grade ammonia is used as the source gas and is further purified by a Nanochem ammonia purifier. The gas enters the MBE chamber through an experimental ammonia cracker cell manufactured by Effusion Science Inc. The cracker cell was designed with a Re filament and fits inside a standard effusion cell sleeve (2.25" diameter) [3]. All substrates were cleaned by a standard degreasing and RCA cleaning procedure prior to loading into the system. Additionally, the substrates were degassed at 700°C for 30 minutes prior to transferring to the deposition chamber.

Reflection high-energy electron diffraction (RHEED) was used to determine the crystalline quality of the films. Scanning electron microscopy (SEM) was used to analyze the films microstructures, and photoluminescence analysis was performed on the GaN films.

C. Results and Discussion

Figure 1 shows the resulting surface morphologies of deposited GaN grown at 800° C using either ammonia cracked directly on the surface of the substrate, or precracked in the ammonia cracker cell as well as the substrate surface.

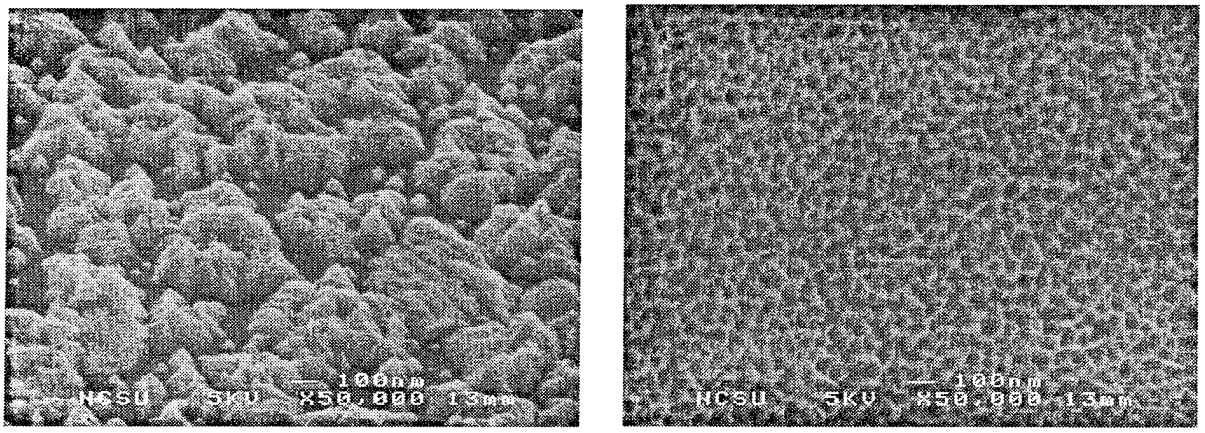

a) b)

Figure 1. Comparison of GaN grown a) with precracked NH_3, and b) without precracked NH_3.

SEM image analysis of the GaN reveals smoother surface morphologies and enhanced growth rates were achieved when growth was performed without precracking the ammonia prior to cracking on the substrate. It is suspected that the reduced growth rate resulting from precracking occurs due to an effective reduction of NH radicals reaching the substrate surface.

RGA characterization of the cracker cell revealed that the primary constituents of the cracked ammonia flux were N_2 and H_2, most likely resulting from recombination of NH molecules leaving the surface of the Re filament. N_2 and H_2 do not contribute to film growth, and thus the only relative source of NH radicals available are those produced from cracking on the substrate surface of any ammonia not previously cracked by the cracker cell.

Figure 2 shows the PL spectrum of GaN grown using ammonia as the nitrogen source. Prior PL of our GaN grown by ECR assisted GSMBE has resulted only in defect peaks and deep level emission. By switching over to ammonia as the nitrogen source, we have for the first time achieved PL emission near the band edge, 354 nm.

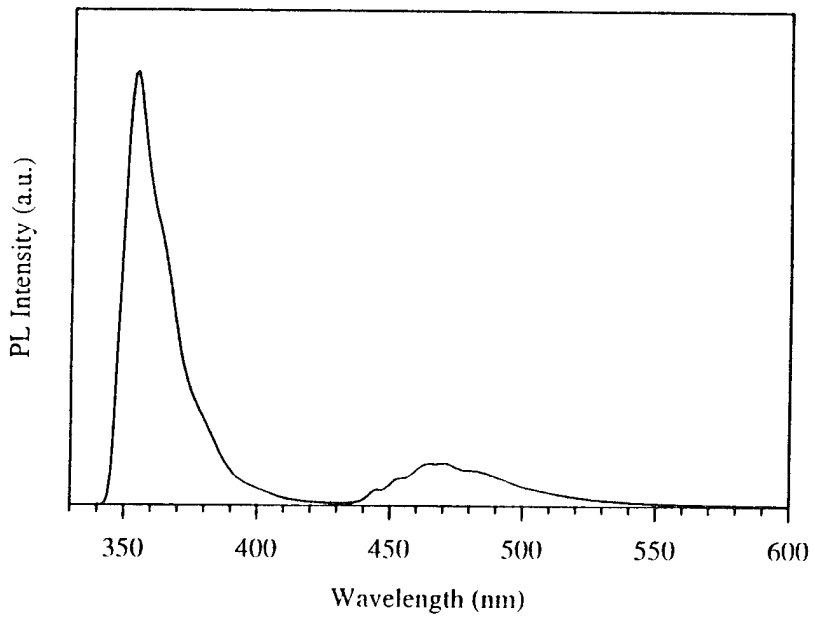

Figure 2. PL of GaN at 8K.

Figure 3 shows the results of SEM analysis performed on AlN grown using ammonia (with and without the assistance of precracking) as the source for nitrogen. In this case, no difference in either surface morphology or growth rate was found using the two methods. Further analysis by TEM may be used in the future to determine this issue. However, by using ammonia instead of the ECR plasma source, we were able to increase our growth rate from 1000A/hr with the ECR, to 3000A/hr with the ammonia.

D. Conclusions

The use of ammonia (NH_3) thermally cracked on the substrate surface (6H-SiC) has lead to a marked improvement in the optical properties of GSMBE grown GaN as characterized by the

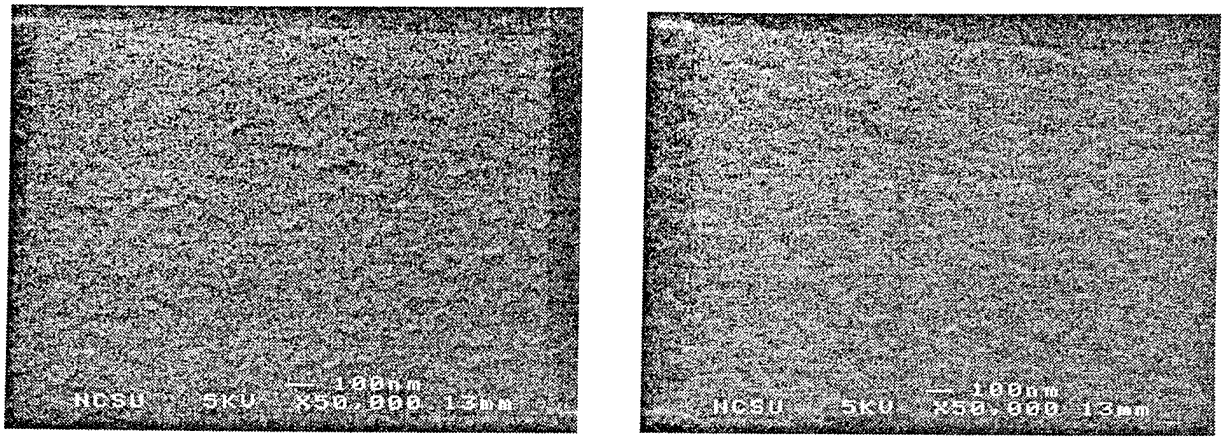

a) b)

Figure 3. Comparison of AlN grown a) with precracked NH_3, and b) without precracked NH_3.

PL spectrum exhibiting a sharp peak at 354 nm in our films for the first time. By using NH_3 as an alternative source for the ECR, the growth rate of AlN has increased from 1000A to 3000A an hour.

The use of a high-temperature ammonia-cracking source to precrack the ammonia has resulted in the degradation of both the film morphology and growth rate for GaN. The effects of the cracker cell on AlN growth is still inconclusive. Analysis of RGA spectra reveal that molecular nitrogen and hydrogen are the primary constituents resulting from decomposition of the ammonia. Recombination of NH molecules leaving the Re filament surface are thought to be the source of the N_2 and H_2. This subsequently leads to a reduced growth rate for GaN films.

E. Future Research Plans and Goals

Over the next few months, further improvement of the GaN film quality will be studied by incorporating the use of AlN and AlGaN buffer layers. We will continue to optimize the quality (microstructurally, optically, and electrically) of our GaN, AlN and their solid solutions grown by using ammonia as the source of the group V species. We will then investigate methods of doping the films to obtain n- and p-type carriers. Once we have established these abilities, we will begin studies aimed at precise *in situ* film thickness monitoring. This will be necessary for fabrication of the Fabry-Pérot cavity and DBR mirrors necessary for efficient lasing of the VCSEL structures.

The possibility of using a nitride to replace the Re filament is under consideration at this time. This may allow for an increase in the ratio of atomic N and NH radicals produced by the

ammonia cracker which will be required for the efficient growth of InN grown at lower growth temperatures.

F. References

1. T. Miyamoto, T. Uchida, N. Yokouchi and K. Iga, J. Crystal Growth **136**, 210 (1994).
2. Y. M. Houng, M. R. T. Tan, B. W. Liang, S. Y. Wang, L.Yang and D. E. Mars, J. Crystal Growth **136**, 216 (1994).
3. Effusion Science Inc., 1994.
4. K. Hirosawa, K. Hiramatsu, N. Sawaki and I. Akasaki, Jpn. J. Appl. Phys. **32**, L1039 (1993).
5. S. Yoshida, S. Misawa and S. Gonda, J. Appl. Phys. **53**, 6844 (1982).
6. C. Wang and R. F. Davis, Appl. Phys. Lett. **63**, 990 (1993).
7. S. Nakamura and T. Mukai, Jpn. J. Appl. Phys. **31**, L1457 (1992).
8. T. Nagatomo, T. Kuboyama, H. Minamino and O. Omoto, Jpn. J. Appl. Phys. **28**, L1334 (1989).
9. M. A. Khan, J. M. Van Hove, J. N. Kuznia and D. T. Olson, Appl. Phys. Lett. **58**, 2408 (1991).
10. N. Yoshimoto, T. Matsuoka, T. Sasaki and A. Katsui, Appl. Phys. Lett. **59**, 2251 (1991).
11. S. Nakamura, M. Senoh and T. Mukai, Jpn. J. Appl. Phys. **30**, L1708 (1991).
12. J. Sumakeris, Z. Sitar, K. S. Ailey-Trent, K. L. More and R. F. Davis, Thin Solid Films **225**, 244 (1993).
13. S. Nakamura, P. Mukai, M. Senoh, Jpn. J. Appl. Phys. **31**, L139 (1992).
14. I. Akasaki, H. Amano, N. Koide, M. Kotaki and K. Manabe, Physica B **185**, 428 (1993).
15. N. Koide, H. Kato, M. Sassa, S. Yamasaki, K. Manabe, M. Hashimoto, H. Amano, K. Hiramatsu and I. Akasaki, J. Crystal Growth **115**, 639 (1991).
16. Semiannual Technical Report, Grant #N00014-90-J-1427.
17. Semiannual Technical Report, Grant #N00014-92-J-1720.

III. Deposition of GaN Thin Films using Supersonic Jet Technology

A. Introduction

The potential optoelectronic applications of wide bandgap materials have stimulated considerable research concerned with thin film growth, characterization and device development of the III-V nitrides, namely cubic BN, AlN, GaN and InN. Of this family GaN has been the most thoroughly studied. Measures of the potential of GaN are revealed by the high Johnson's and Keye's figures of merit of 80.0×10^{11} and 4.2×10^{8}, respectively, compared to 4.75×10^{11} and 2.39×10^{8} for silicon[1]. Gallium nitride usually forms in the wurtzite structure with a bandgap of 3.4 eV[2]. However, several groups[3-6] have deposited films of the cubic (zincblende structure) β-GaN which has a smaller bandgap of 3.26 eV. As the wurtzitic polytype of GaN forms continuous solid solutions with both AlN and InN which have bandgaps of 6.2 eV[7] and 1.9 eV[8], respectively, materials having engineered bandgaps may be produced for the construction of optoelectronic devices that are active from the visible to the deep ultraviolet frequencies.

A major difficulty in the growth of thin films of GaN is the lack of suitable substrates. The lattice parameters and coefficients of thermal expansion are given in Table I for GaN and the most common substrate materials of Si, SiC (6H and 3C), sapphire, ZnO and GaAs. With the possible exception of the basal planes of α(6H)-SiC and ZnO, none of these materials are suitable for the two-dimensional epitaxial growth of GaN.

Table I. Physical Properties of GaN and Potential Substrate Materials[3]

Material	Lattice Parameter	Coefficient of Thermal Expansion
GaN	a = 3.189 Å	5.59×10^{-6} K^{-1}
	c = 5.185 Å	3.17×10^{-6} K^{-1}
Si	a = 5.43Å	3.59×10^{-6} K^{-1}
α-SiC (6H)	a = 3.08 Å	4.2×10^{-6} K^{-1}
	c = 15.12 Å	4.7×10^{-6} K^{-1}
β-SiC (3C)	a = 4.36 Å	2.7×10^{-6} K^{-1}
Al_2O_3	a = 4.758 Å	7.5×10^{-6} K^{-1}
	c = 12.991 Å	8.5×10^{-6} K^{-1}
GaAs	a = 5.653 Å	6.0×10^{-6} K^{-1}

To reduce thermal budgets and permit finer scale architecture, low GaN deposition temperatures are highly desirable. However, as deposition temperature is reduced, the surface mobility of deposition precursors is curtailed and film crystallinity and morphology are compromised. In addition to decreased surface mobility, another difficulty with low temperature GaN deposition is that the source materials, TEG and NH_3, decompose at greatly different temperatures. As the NH_3 molecule is more stable than the triethylgallium molecule, a mechanism to enhance the reactivity of ammonia is desirable.

Seeded supersonic beams may potentially drive the reaction and dissociative chemisorption of NH_3 on select substrates. By increasing the kinetic energy of the seeded molecules, a substantial amount energy can be carried by each molecule that can drive surface reactions when the molecule strikes the substrate surface. Engstrom *et al.*[10] have determined that the reaction probability of Si_2H_6 on the Si(100) increases rapidly for incident supersonic beam energies above about 23 kcal mol^{-1}. This effect may be applied to the reaction of NH_3 on selected substrate.

The objective of this research is to develop techniques for depositing GaN films using seeded supersonic jets. The immediate goal is to produce GaN films at reduced temperatures and determine the effect of varying deposition conditions on film character. Toward this end, GaN with an existing single jet system are being studied to determine ranges of growth parameters for GaN film deposition that can be used in a dual beam system now under construction.

B. Experimental Procedure

Sample Cleaning. Si(100) and Si(111) substrates were cleaned in a three step process: First the substrates were immersed in a 10% HF solution for 1 minute to remove the native oxide. Next, the samples were exposed in air to ultra violet light to oxidize the surface. After the illumination, the substrates were again immersed in the 10% HF solution prior to loading into the reactor.

Al_2O_3(0001) substrates were cleaned via a multiple step process. Firstly, the samples were successively ultrasonically cleaned in trichloroethylene, acetone and methanol. After water rinsing, the samples were immersed in a 70°C, 50:50 mixture of H_3PO_4 and H_2SO_4 for 5 minutes. After water rinsing, the substrates were finally immersed in a 10% HF solution immediately prior to installation in the reactor.

Deposition Reactor. A schematic of the single beam deposition system is presented in Fig. 1. This system may be operated in either of two modes depending on whether a skimmer is installed. All work up to this point has been conducted in the free jet mode where a skimmer is not installed.

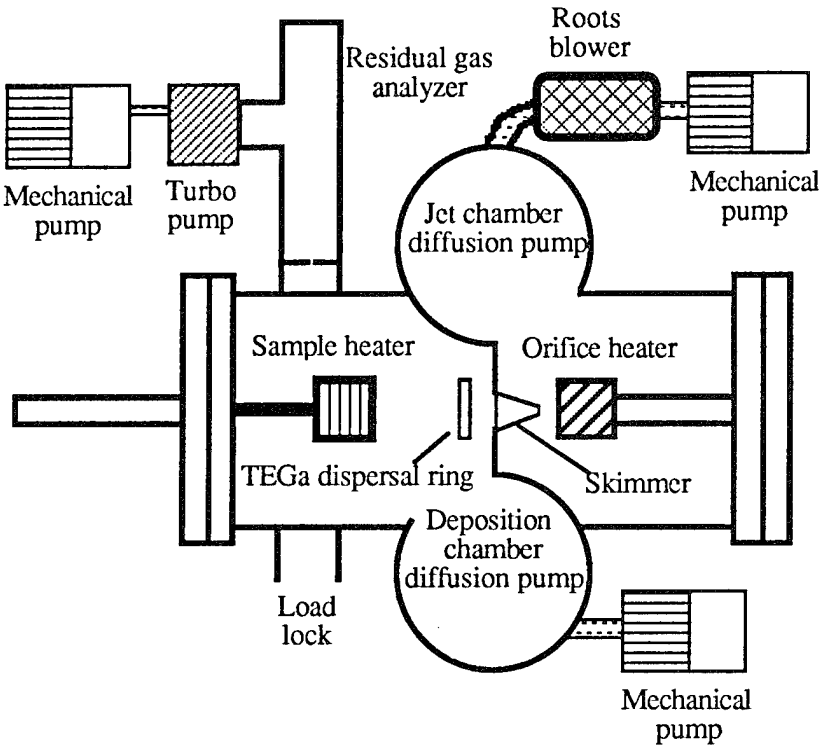

Figure 1. Single beam supersonic jet deposition system.

Deposition. After installation in the reactor, the samples are heated to the deposition temperature while a 5% NH_3 in He gas flow is maintained through the reactor. Typical deposition conditions are listed in Table II. As indicated in the table, although the total flow rates may vary, an NH_3 to TEG ratio of ≈200 has been found to produce the best films. After deposition, the TEGa flow is terminated and the sample is cooled to <200°C under flowing NH_3 /He.

Table II. Typical GaN deposition conditions

Parameter	Value
Substrate temperature	540°to 580°C
Orifice pressure	600 to 1000 Torr
Orifice temperature	510°C
Orifice gas	5% NH_3 in He
TEG bubbler temperature	-5 to 10°C
TEG bubbler pressure	800 Torr
TEG carrier	5 to 40 sccm He
NH_3/ TEG ratio	≈200

C. Results and Discussion

Film Deposition. Stoichiometric GaN films can be produced across the range of process variables listed in Table II. A scanning electron micrograph of a GaN film deposited on a Si(111) substrate is presented in Fig. 3. This film was deposited at 560°C and exhibited excellent thickness uniformity and minimal surface roughness. Figure 4 is a scanning electron micrograph of a GaN film deposited on an Al_2O_3(0001) substrate under conditions identical to those for the film in Fig. 3. This latter film was not of uniform thickness and has a much more irregular surface.

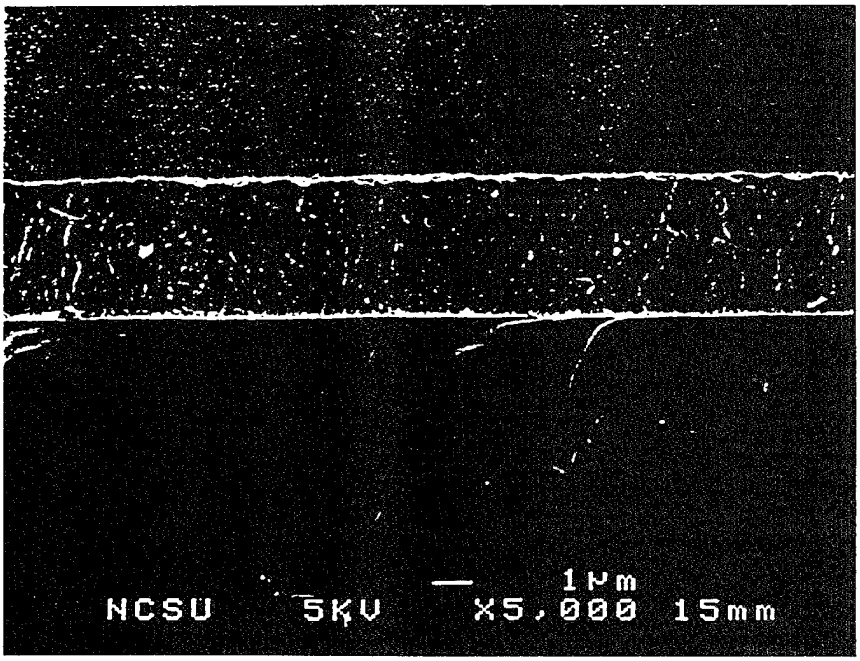

Figure 3. GaN film deposited on Si(111) substrate.

Auger electron spectroscopy revealed that C and O are the major contaminants in the deposited GaN films. Figure 5 compares three spectra take from a GaN film before sputtering, after Ar ion sputtering for 60 seconds and finally after sputtering for 120 seconds total. A reduction in the C and O content after the initial 60 second sputter is indicated in the figure. This is consistent with the removal of a surface contamination layer. The supersonic beam deposition chamber is not connected to the Auger analysis chamber, precluding *in vacuo* transfers and necessitating an in-air transfer that exposes the samples to contaminants.

The spectrum collected after 120 seconds of Ar ion sputtering shows significant C contamination. This last spectrum also shows the presence of Si, indicating that most of the GaN film had been milled away revealing the Si substrate. The fine structure of the C peak is consistent with graphitic C and not SiC. The presence of the C at the film/substrate interface is attributed to C contamination in the deposition system. The chamber is pumped by oil diffusion pumps and oil contamination is always a concern.

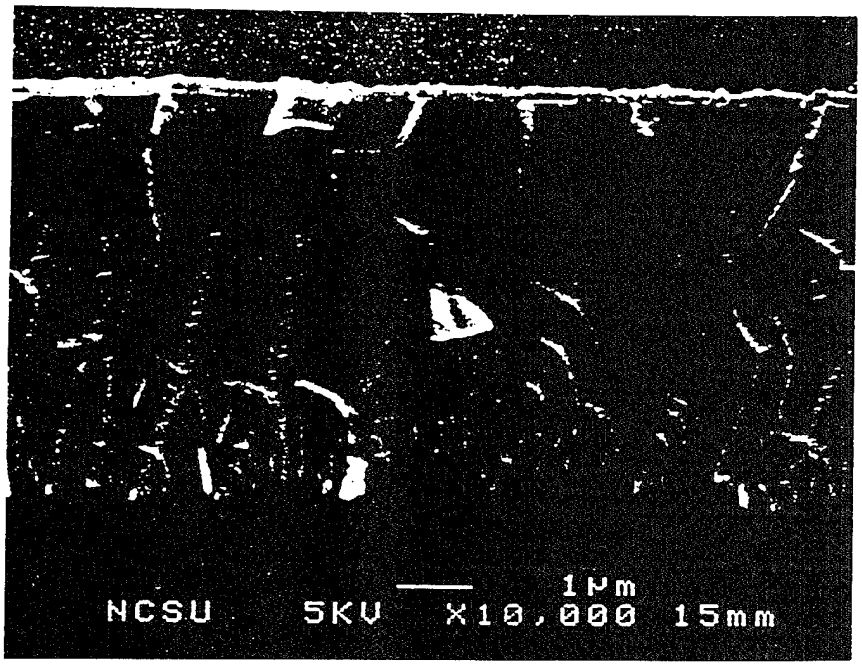

Figure 4. GaN film deposited on $Al_2O_3(0001)$ substrate.

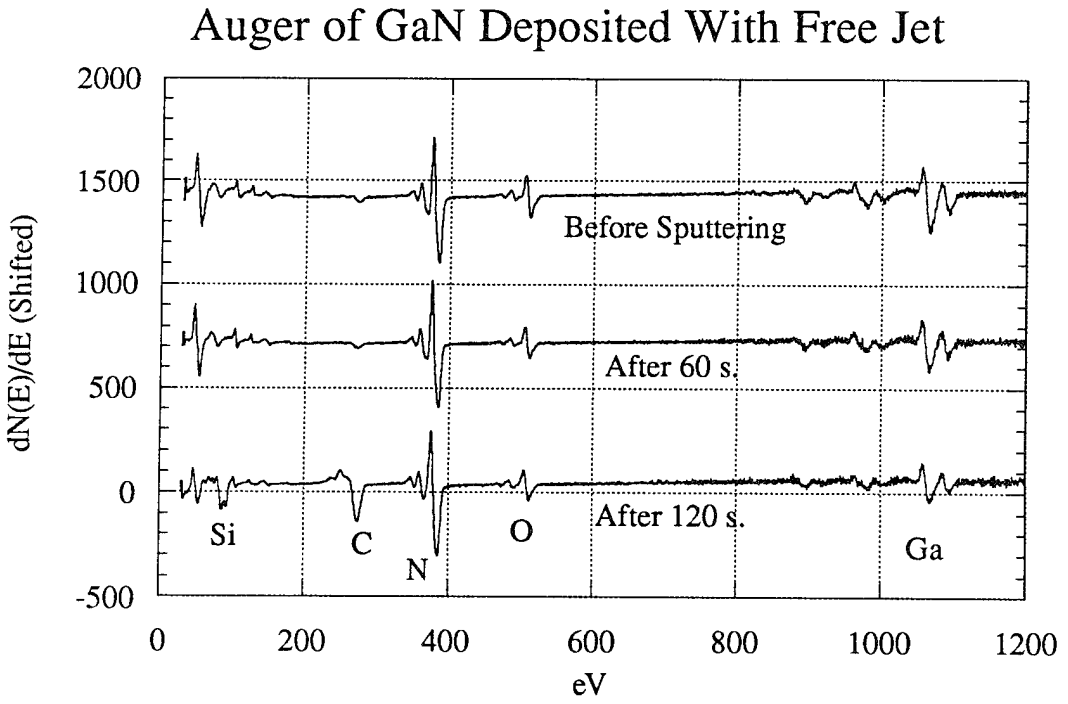

Figure 5. Auger electron spectra collected from GaN film before and after Ar ion sputtering.

System Design. A dual seeded supersonic beam deposition system is currently under construction. This system will contain five chambers: load lock, sample transfer line, beam source chamber, deposition chamber and analysis chamber. A schematic overview of the system is presented in Fig. 6.

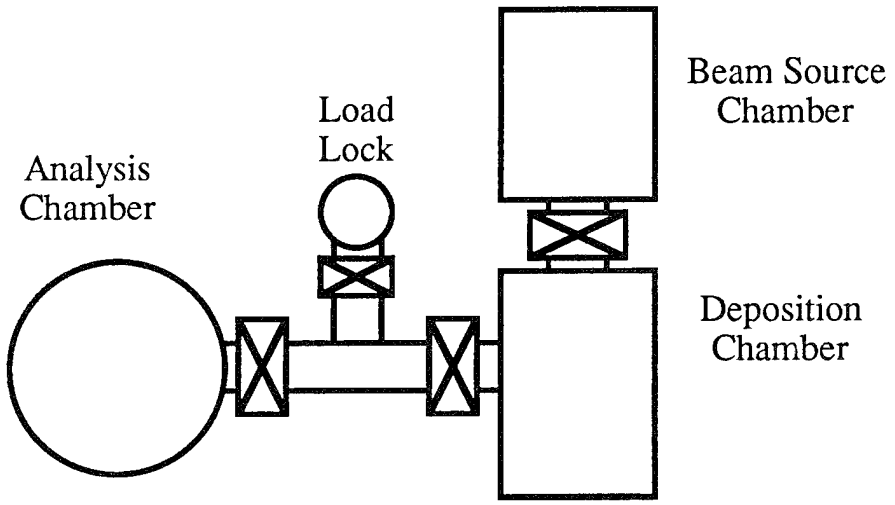

Figure 6. Schematic of dual beam deposition system and analysis chamber.

Samples may be moved through the system as follows:

After the installation of samples, the load lock will be evacuated by a Drytel 31 combination molecular drag-diaphram pump to $<10^{-5}$ Torr before samples can access the sample transfer line.

The sample transfer line is evacuated by a Cryo-pump and permits the movement of samples between the deposition chamber and the analysis chamber under $<10^{-8}$ Torr vacuum.

The deposition chamber is connected to the transfer line and the beam source chamber. A heater stage in this chamber can achieve sample temperatures of ≈600°C. This chamber also contains a RHEED system and a mass spectrometer mounted on a rotatable stage. The mass spectrometer may be configured to perform time of flight measurements of the seeded beams as well as being used for residual gas analysis. Pumping of the deposition chamber will be accomplished with a magnetically levitated combination turbomolecular-molecular drag pump backed by a Fomblinized mechanical pump and an available cryo-cooled titanium sublimation pump. Up to four Knudsen evaporation cells may be fitted to this chamber in addition to an Oxford style R.F. plasma source. Once completely equipped, this versatile chamber may be employed for many varieties of sample cleaning and film deposition processes.

The beam source chamber is divided into two stages: a source stage and a differential pumping stage. Heated nozzles in the first stage generate the supersonic beams which pass through skimmers into the differential pumping stage where the beams are collimated. The

differential pumping stage contains beam flags to interrupt the beams and chopper wheels that may be employed to generate a pulsed beam for time of flight measurements. The collimated beams then are directed into the deposition chamber where they are coincident on the substrate.

The last chamber in the new system is an ultra-high vacuum deposition chamber. The primary analysis technique to be performed in this chamber will be X-ray photoelectron spectroscopy with an angle resolved capability. The configuration of this chamber will also permit the performance of reflectance infrared spectroscopy. This chamber is evacuated by an Ion pump.

D. Conclusions

1. General conditions favoring the deposition of GaN films from a free jet source on Si(111) and Al_2O_3(0001) substrates have been determined.
2. C and O are the major contaminants found in the GaN films.
3. The C and O contaminant appear to be present in the highest concentrations on the film surface and at the film/substrate interface. Inadequate system cleanliness and in-air transfers have been identified as major contaminating agents.
4. A dual beam deposition system has been largely designed and is currently under construction. This versatile system will have the capability of depositing films from dual seeded beams or from a selection of sources including Knudsen cells, gas sources and plasma-assisted gas sources. The system will also offer the capability of performing time of flight measurements, desorption studies, RHEED characterization, XPS, angle resolved XPS and reflectance spectroscopy.

E. Future Plans

1. Install skimmer into single beam system and develop conditions for depositing GaN films using a skimmed, NH_3 seeded He beam.
2. Install TEG jet source in single beam system in an attempt to deposit GaN films with a combination skimmed, NH_3 seeded He beam and free TEG seeded He beam.
3. Continue the design and construction of dual seeded beam deposition system.

F. References

1. J. H. Edgar, J. Mater. Res. **7**, 235 (1992).
2. H. P. Maruska and J. J. Tietjen, Appl. Phys. Lett. **15**, 327 (1969).
   701 (1989).
3. M. J. Paisley, Z. Sitar, J. B. Posthill and R. F. Davis, J. Vac. Sci. and Technol. B **7**, 701 (1989).
4. S. Strite, J. Ruan, Z. Li, A. Salvador, H. Chen, D. J. Smith, W. J. Choyke and H. Martoc, J. Vac. Sci. and Technol. B **9**, 1924 (1991).
5. T. Lei, M. Fanciulli, R. J. Molnar and T. D. Moustakas, Appl. Phys. Lett. **59**, 944 (1991).

6. M. Mizuta, S. Fujieda, Y. Matsumoto and T. Kawamura, Jpn. J. Appl. Phys. **25**, L945 (1986).
7. W. M. Yim, E. J. Stofko, P. J. Zanzucchi, J. I. Pankove, M. Ettenberg and S. L. Gilbert, J. Appl. Phys. **44**, 292 (1973).
8. J. A. Sajurjo, E. Lopez-Cruz, P. Vogh and M. Cardona, Phys. Rev. B **28**, 4579 (1983).
9. H. P. Naruska, D. A. Stevens and J. I. Pankove, Appl. Phys. Lett. **22**, 303 (1973).
10. J. R. Engstrom, D. A. Hansen, M. J. Furjanic and L. Q. Xia, J. Chem. Phys. **99**, 4051 (1993).

IV. Fabrication and Characterization of MIS Diodes of Al/AlN/SiC by Gas-Source Molecular Beam Epitaxy

A. Introduction

Silicon carbide (SiC) is a wide band gap material that makes it attractive for the fabrication of electronic devices that operate in a variety of harsh environments. SiC has a wide band gap (≈3.0 eV at room temperature), excellent thermal stability[1-3], a high thermal conductivity (4.9 W $cm^{-1}K^{-1}$)[4], a high breakdown field (2×10^6 V cm^{-1})[2] and a high saturated electron drift velocity (2×10^7 cm s^{-1})[3]. In the last few years, blue light emitting diodes (LEDs), junction field effect transistors (JFETs) and metal-oxide-semiconductor field effect transistors (MOSFETs) have become commercially available. Excellent reviews of these devices have been published[5-11].

Since metal-insulator-semiconductors (MIS) structures are an important part of today's microelectronics industry, MIS diodes (using SiO_2, in particular, as the insulator) have been studied by a number of researchers. The majority of the studies have been done on 6H-SiC substrates. Although some work[12-16] has also been done on 3C-SiC, the defective nature of the material make most of the measurements difficult to interpret since the resulting interface state densities and fixed oxide charge densities were very high. Most of this work has centered around the optimization of the oxidation both kinetically and electrically; however, the chemical character of the oxide has also been studied by Auger electron spectroscopy[17, 18] and secondary ion mass spectroscopy[16, 19, 20]. Nearly all reports (see for example[21]) report that the MOS diodes can be easily accumulated and depleted at room temperature; however, inversion can only be obtained when the samples are illuminated by a UV light. The lowest reported values[22] of fixed charge densities and interface state densities are 9×10^{11} cm^{-2} and 1.5×10^{11} cm^{-2} eV^{-1}, respectively. To date, there has only been one report[23] of a MIS diode made with an insulator other than SiO_2. In this case, Si_3N_4 was used, but had only minimal success due to very large density of defects and large leakage currents.

Aluminum nitride possesses a direct band gap of 6.28 eV at 300 K[24], a melting point in excess of 2275 K[25] and a thermal conductivity of 3.2 W cm^{-1} K^{-1}[26] As such, it is a candidate material for high-power and high-temperature microelectronic and optoelectronic applications with the latter employment being particularly important in the ultraviolet region of the spectrum[24]. These properties strongly indicate that superior surface acoustic wave devices, operational in aggressive media and under extreme conditions both as sensors for high temperatures and pressures and as acousto-optic devices can be developed[27-29]. However, progress regarding these (and other) applications is hampered by the lack of good single crystal material.

B. Experimental Procedure

Thin, epitaxial films of several thicknesses of AlN were grown on a variety of Si-face α-SiC(0001) substrates supplied by Cree Research, Inc. The different α-SiC(0001) wafers are listed in Table I. Each of the wafers contained a 0.8 μm epitaxial SiC layer deposited via CVD and a thermally oxidized 75 nm layer to aid in wafer cleaning. The surfaces were prepared by a 10% HF dip and a 10 minute anneal at 1050 °C in UHV as well as a silane exposure and boil-off described in previous reports.

Table I. SiC Substrates used in this Research

on-axis, n-type ($n = 2.8 \times 10^{16}$ cm^{-3}) 6H-SiC
off-axis, n-type ($n = 2.4 \times 10^{16}$ cm^{-3}) 6H-SiC
off-axis, p-type ($n = 2.1 \times 10^{16}$ cm^{-3}) 6H-SiC
off-axis, n-type ($n = 5.0 \times 10^{15}$ cm^{-3}) 4H-SiC

All growth experiments were carried out in the gas-source molecular beam epitaxy system detailed in previous reports. Films of AlN were grown at 1100 °C. Source were aluminum (99.9999% purity), evaporated from a standard MBE effusion cell operated in all cases at 1150°C, and 7.0 sccm ammonia (99.999% pure). Typical base pressures of 10^{-9} Torr were used. Aluminum contacts (area = 5×10^{-3} cm^2) were deposited on the AlN by means of a standard evaporator and In-Sn solder was used a contact to the SiC.

High frequency capacitance-voltage measurements were performed on a HP 4275A C-V analyzer and the quasistatic C-V and I-V measurements were performed on a HP 4140B analyzer. Measurements were performed with the assistance of S. Cohen of IBM T. J. Watson Research Center in Yorktown Heights, NY. These analyzers were programmed to measure C-V and I-V characteristics of the diodes as well as to calculate the insulator thickness from the capacitance. Measurements were performed on diodes with AlN thicknesses of 1000 Å and 2500 Å.

C. Results

In all cases, the diodes could be accumulated and depleted with the application of small gate voltages. Figure 1 shows C-V curves for a typical 1000 Å sample. However, deep depletion and inversion were not achieved in any case. For the 1000 Å samples, the leakage current was too high to accurately measure quasistatic C-V response.

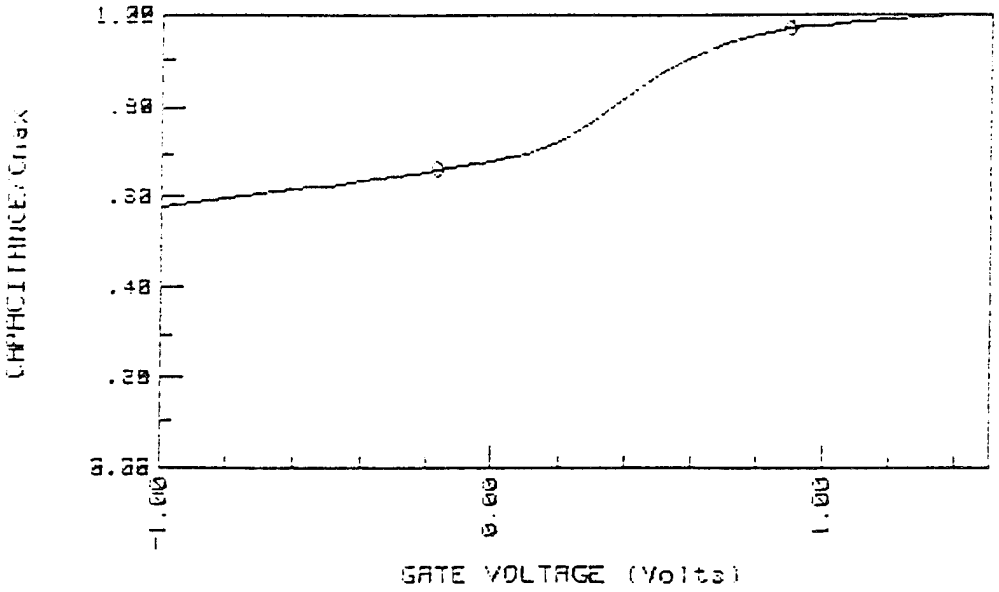

Figure 1. High frequency C-V curve for a typical Al/AlN/SiC diode. The AlN thickness is 1000 Å.

The leakage current was reduced by increasing the AlN thickness to 2500 Å. In this case, both the high frequency and the quasistatic C-V curves were measured. Figure 2 shows both of these curves on the same graph. At this thickness, the samples had low leakage currents (Fig. 3) but still did not undergo inversion.

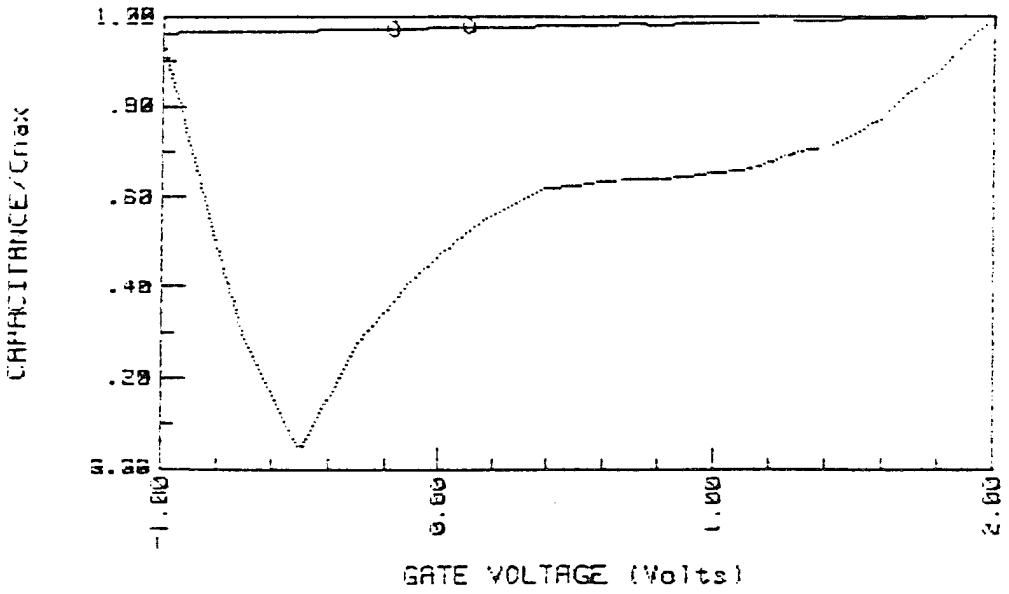

Figure 2. High frequency (solid line) and quasistatic (dotted line) C-V curves for an Al/AlN/SiC diode. The AlN thickness is 2500 Å.

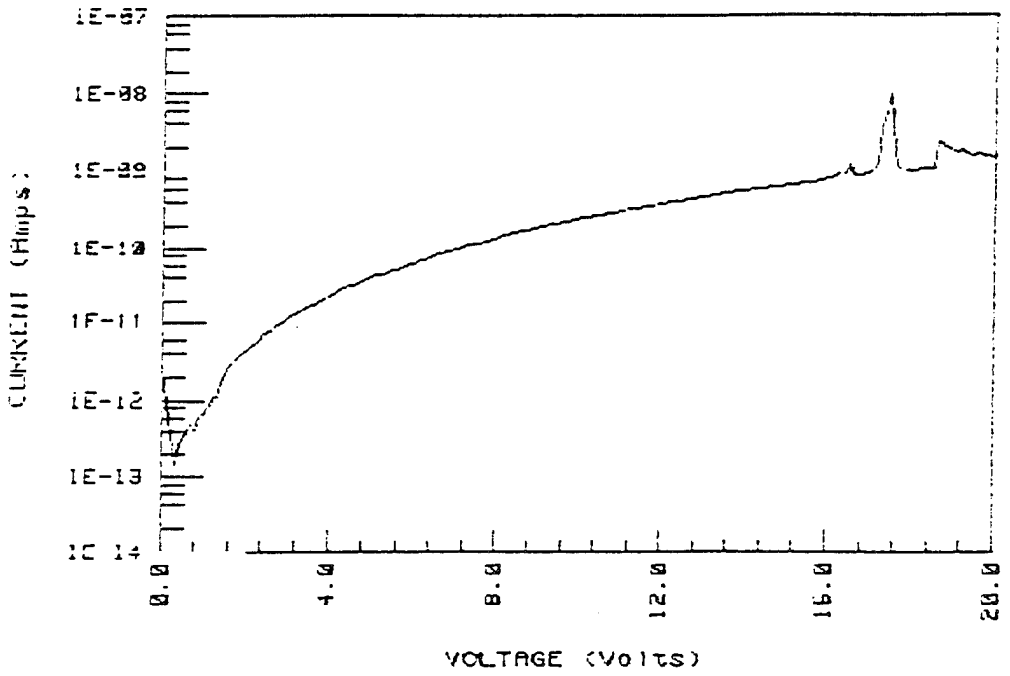

Figure 3. I-V curve for an Al/AlN/SiC diode. The AlN thickness is 2500 Å.

An interesting result of this work was that the capacitance showed a large dependency on applied frequency. When different frequencies were applied, the measured insulator capacitance was different each frequency.

D. Discussion

Figures 1 and 2 show the accumulation and depletion of Al/AlN/SiC diodes. Attempts to invert these samples at room temperature were unsuccessful. This is due to several factors. The extremely low intrinsic carrier concentration in SiC ($\approx 10^{-6}$ cm^{-3}) and the low carrier generation significantly reduce the number of minority carriers available in the SiC surface region. Despite the inability to measure the interface state density due to the leakage in the insulator, the presumed high concentration of these states as well as traps and defects in the SiC (independent of the AlN insulator) may also prevent inversion. Thicker AlN layers show better leakage characteristics and may be necessary to achieve excellent insulating properties. The dependence of the capacitance on frequency implies a relationship between dielectric constant and frequency as well since the capacitance and the dielectric constant are related by insulator thickness only.

E. Conclusions

Thin AlN insulating layers on SiC have been used in MIS structures. The resulting diodes can be accumulated and depleted but cannot be inverted by high frequency C-V characterization. Layers thinner than 1000 Å are too leaky to perform quasistatic measurements to determine the density of interface states. A large dependency of AlN dielectric constant on frequency was also observed.

F. Future Research Plans and Goals

The first priority is to reduce the leakage current and make accurate measurements of the interface state density. This will be accomplished by growing thicker layers (≈3000 Å) of AlN on the same substrates and repeating the measurements. The second priority is to achieve inversion of the semiconductor. Effects of temperature and illumination will be determined.

G. References

1. R. B. Campbell and H.-C. Chang, in *Semiconductors and Semimetals, Vol. 7B*, edited by R. K. Willardson and A. C. Beer (Academic Press, New York, 1971), p. 625.
2. W. von Muench and I. Pfaffeneder, J. Appl. Phys. **48**, 4831 (1977).
3. W. von Muench and E. Pettenpaul, J. Appl. Phys. **48**, 4823 (1977).
4. G. A. Slack, J. Appl. Phys. **35**, 3460 (1964).
5. R. F. Davis, J. W. Palmour and J. A. Edmond, Mater. Res. Soc. Symp. Proc. **162**, 463 (1990).
6. R. F. Davis, in *The Physics and Chemistry of Carbides; Nitrides and Borides*, edited by R. Freer (Kluwar Academic Publishers, The Netherlands, 1990), p. 589.
7. R. F. Davis, G. Kelner, M. Shur, J. W. Palmour and J. A. Edmond, Proc. IEEE **79**, 677 (1991).
8. R. F. Davis, J. W. Palmour and J. A. Edmond, Diam. Rel. Mater. **1**, 109 (1992).
9. R. F. Davis, Phys. B **185**, 1 (1993).
10. P. A. Ivanov and V. E. Chelnokov, Semicond. Sci. Technol. **7**, 863 (1992).
11. J. A. Powell, P. G. Neudeck, L. G. Matus and J. B. Petit, Mater. Res. Soc. Symp. Proc. **242**, 495 (1992).
12. K. Shibahara, S. Nishino and H. Matsunami, Jpn. J. Appl. Phys. **23**, L862 (1984).
13. R. E. Avila, J. J. Kopanski and C. D. Fung, Appl. Phys. Lett. **49**, 334 (1986).
14. S. M. Tang, W. B. Berry, R. Kwor, M. V. Zeller and L. G. Matus, J. Electrochem. Soc. **137**, 221 (1990).
15. M. Shinohara, M. Yamanaka, S. Misawa, H. Okumura and S. Yoshida, Jpn. J. Appl. Phys. **30**, 240 (1991).
16. C. Raynaud, J.-L. Autran, J.-B. Briot, B. Balland, N. Bécourt and C. Jaussaud, J. Electrochem. Soc. **142**, 282 (1995).
17. R. W. Kee, K. M. Geib, C. W. Wilmsen and D. K. Ferry, J. Vac. Sci. Technol. **15**, 1520 (1978).
18. R. Berjoan, J. Rodriguez and F. Sibieude, Surf. Sci. **271**, 237 (1992).
19. C. Raynaud, J.-L. Autran, B. Balland, G. Guillot, C. Jaussaud and T. Billon, J. Appl. Phys. **76**, 993 (1994).
20. C. Raynaud, J.-L. Autran, F. Seigneur, C. Jaussaud, T. Billon, G. Guillot and B. Balland, J. Phys. III **4**, 937 (1994).
21. A. Rys, N. Singh and M. Cameron, J. Electrochem. Soc. **142**, 1318 (1995).
22. J. N. Shenoy, G. L. Chindalore, M. R. Melloch, J. A. Cooper, Jr., J. W. Palmour and K. G. Irvine, J. Electron. Mater. **24**, 303 (1995).
23. G. E. Morgan, C. C. Tin, J. R. Williams and R. Ramesham, in *Silicon Carbide and Related Materials*, edited by M. G. Spencer, R. P. Devaty, J. A. Edmond, M. A. Khan, R. Kaplan, and M. Rahman (Institute of Physics, Bristol, 1994), p. 645.
24. W. M. Yim, E. J. Stofko, P. J. Zanzucchi, J. I. Pankove, M. Ettenberg and S. L. Gilbert, J. Appl. Phys. **44**, 292 (1973).
25. M. G. Norton, P. G. Kotula and C. B. Carter, J. Appl. Phys. **70**, 2871 (1991).
26. G. A. Slack, J. Phys. Chem. Solids **34**, 321 (1973).
27. J. K. Liu, K. M. Lakin and K. L. Wang, J. Appl. Phys. **46**, 3703 (1975).
28. M. Morita, N. Uesugi, S. Isogai, K. Tsubouchi and N. Mikoshiba, Jpn. J. Appl. Phys. **20**, 17 (1981).
29. G. D. O'Clock, Jr. and M. T. Duffy, Appl. Phys. Lett. **23**, 55 (1973).

V. Distribution List

Mr. Max Yoder Office of Naval Research Electronics Division, Code: 312 Ballston Tower One 800 N. Quincy Street Arlington, VA 22217-5660	3
Administrative Contracting Officer Office Of Naval Research Resident Representative The Ohio State University Research Center 1960 Kenny Road Columbus, OH 43210-1063	1
Director, Naval Research Laboratory ATTN: Code 2627 Washington, DC 20375	1
Defense Technical Information Center Bldg. 5, Cameron Station Alexandria, VA 22314	4